Inorg. Chem. **2004**, *43*, 2803–2809

Hydrogen Bonding in the Crystal Structures of the Ionic Liquid Compounds Butyldimethylimidazolium Hydrogen Sulfate, Chloride, and Chloroferrate(II,III)

Philipp Kölle and Richard Dronskowski*

Institut für Anorganische Chemie, Rheinisch-Westfälische Technische Hochschule, 52056 Aachen, Germany

Received October 27, 2003

Four ionic liquid (IL) salts containing the 1-butyl-2,3-dimethylimidazolium (BDMIM) and 1-allyl-2,3-dimethylimidazolium (ADMIM) cations have been prepared; the characterization was based on IR spectroscopy and single-crystal structure determination. The compounds BDMIM[HSO_4], BDMIMCl, ADMIMBr, and (BDMIM)$_4$[$Fe^{II}Cl_4$][$Fe^{III}Cl_4$]$_2$ were chosen to incorporate anions significantly differing in hydrogen-bond-acceptor strength in order to elucidate the influence of directional bonding on crystal packing. The cations adopt different arrangements with respect to the counterions. The role of hydrogen bonding in these compounds is discussed with respect to its general significance for lattice energies of IL salts.

1. Introduction

Since the importance of medium and weak hydrogen bonding in extended molecular networks has been recognized and rationalized in terms of topology, bond strength, and its predictive value for crystal engineering, the geometry of the D−H···A (D, donor; A, acceptor) arrangement has gained importance over pure distance criteria.[1,2] It was Taylor and Kennard who first showed in a statistical evaluation of more than 100 Cambridge Structural Database (CSD) structures determined by neutron diffraction that C−H···X contacts (X = O or Cl) below the sum of the van der Waals radii are found much more frequently than C−H···H and C−H···C contacts.[3] They also found the distribution of C−H···X angles to be indicative of a high preference for directional bonding. The main contribution to the hydrogen-bond energy is Coulombic interaction between the positive and negative partial charges on the hydrogen atom and the acceptor atom, respectively. This contribution will be especially strong for charge-assisted hydrogen bonds which are present in ionic liquid (IL) salts. Although there appears to be no case in the literature where IL model compounds have been submitted to neutron diffraction for structural investigation, the existence of hydrogen bonds can be unambiguously inferred from the C−X and the approximate H···X distances together with the C−H···X angle. Recently, the C−H···Cl hydrogen bond has been investigated by statistical analysis of bond lengths and angles of several hundred CSD crystal structures by Aakeröy et al.[2] The authors found the most frequent abundance of C−H···Cl^- contacts at distances greater than the conventional van der Waals cutoff. An equation relating the charge density on each atom in the anion to the total charge of the ion has been previously derived;[4] it is given in eq 1:

$$\rho = \frac{z^2}{n} \leq 1 \qquad (1)$$

The charge density (ρ) is approximated by the square of the total charge of the ion (z^2) divided by the number of atoms (n) on which this charge is delocalized. With chlorometalate anions, substantial hydrogen bonding with imidazolium ring hydrogen atoms has been previously found to be virtually absent if the charge density is smaller than 1. This appears to be equally true for the anions [BF_4^-], [PF_6^-], and [SbF_6^-].[5] The above equation, however, does not generally hold for oxo-anions which is obvious by comparing the crystal structures and melting points of EMIM[NO_3],

* Author to whom correspondence should be addressed. E-mail: drons@HAL9000.ac.rwth-aachen.de.

(1) Desiraju, G. *Acc. Chem. Res.* **2002**, *35*, 565.
(2) Aakeröy, C. B.; Evans, T. A.; Seddon, K. R.; Palinko, I. *New. J. Chem.* **1999**, 145.
(3) Taylor, R.; Kennard, O. *J. Am. Chem. Soc.* **1982**, *104*, 5063.
(4) Elaiwi, A.; Hitchcock, P. B.; Seddon, K. R.; Srinivasan, N.; Tan, Y.-M.; Welton, T.; Zora, J. A. *J. Chem. Soc., Dalton Trans.* **1995**, 3467.
(5) Kölle, P.; Dronskowski, R. *Eur. J. Inorg. Chem.*, in press.

10.1021/ic035237l CCC: $27.50
Published on Web 04/07/2004

published by Wilkes and Zaworotko in 1992,[6] and BDMIM-[HSO_4], prepared in the course of this work.

With three hydrogen atoms bound to the imidazolium ring, two or three resolved absorption bands are observed with 1-alkyl-3-methylimidazolium salts in the IR spectral region between 3000 and 3200 cm^{-1}. These can be attributed to coupled aromatic C−H stretching vibrations. Several authors have inferred the existence of strong hydrogen bonds between these hydrogens and basic counterions such as halides from red shifts of the aromatic ν(C−H) absorption bands, as compared to spectra with weakly basic counterions such as [$AlCl_4^-$] and [$AlBr_4^-$].[4,7] The existence of hydrogen bonding in ionic liquid salts has been unambiguously established in the crystal structures of all EMIMX salts (X = Cl, Br, or I)[4] and the compounds [EMIM]$_2$[MCl_4] and [Me_2EtIm]$_2$[MCl_4] (M = Co or Ni).[8,9] All these compounds have melting points above 350 K. Nonetheless, hydrogen bonding can also be identified in the crystal structure of EMIM[NO_3].[6] This compound has a reported melting point of only 311 K, but three short contacts of the type discussed before are found in the structure.

Additional evidence for hydrogen bonding in neat liquid salts, and solutions of these in organic solvents, comes from investigations of NMR chemical shifts of the ring protons where downfield shifts are indicative of hydrogen bonding. The situation in the liquid state is, however, complicated by concomitant ion pairing and π-stacking of the aromatic rings, which causes an upfield shift for protons extending into the shielding region of the neighboring cation.[10,11]

Suarez et al. claimed the existence of C−H···F hydrogen bonds in liquid BMIM[BF_4] and BMIM[PF_6] from observed red shifts of the aromatic C−H stretching bands in the IR spectra.[12] This conclusion has been corroborated by Huang et al. and Mele et al. in NMR studies of liquid EMIM[BF_4] and has been attributed to the formation of C(2)−H···F bonds.[13,14]

In this work, we demonstrate how hydrogen bonding is effective in three different IL compounds containing anions of substantially different hydrogen-bond-acceptor strength. IL chlorides and bromides have been used as solvents in some applications at rather high temperatures around 100 °C. IL hydrogen sulfates and alkyl sulfates are currently explored as alternative solvents to potentially corrosive fluoro anions.[15] IL chloroferrates are investigated due to their chemical similarity with the first and most extensively studied chloroaluminates. From the latter class of compounds, no example of a crystal structure has yet been reported. However, Elaiwi et al. have communicated the crystal structure of EMIM[$AlBr_4$].[4] The influence of hydrogen bonding exerted by the imidazolium cation on the endo/exo selectivity of Diels−Alder reactions[16] and the rate of neutral allylic substitutions[17] carried out in BMIM ionic liquids have recently been reported. In this work, hydrogen bonding is clearly shown to be the dominating force which determines packing of the ions in the crystal lattices and by far exceeds the contributions of Coulombic and dispersive forces. The structural evidence is supported by the ν(C−H) infrared shift criterion in all cases.

2. Experimental Section

2.1. Preparations. BDMIMCl was obtained from *n*-chlorobutane and 1,2-dimethylimidazole (Aldrich 98%) as previously reported.[18] 1-Allyl-2,3-dimethylimidazolium bromide was synthesized from allyl bromide and 1,2-dimethylimidazole using the same procedure. The highly hygroscopic compounds were characterized by NMR and IR spectroscopy and elemental analysis. Colorless crystals suitable for X-ray single-crystal diffraction were obtained from supersaturated solutions of the salts in dry acetone. The melting point was determined to be 100(±1) °C.

(BDMIM)$_4$[$Fe^{II}Cl_4$][$Fe^{III}Cl_4$)]$_2$ was prepared by mixing the anhydrous chlorides BDMIMCl, $FeCl_3$, and $FeCl_2$ in a molar ratio of 4:2:1 and stirring at 50 °C for some time until a homogeneous melt had formed. The yellow-green, nonhygroscopic compound solidifies upon cooling to ambient temperature. The compound was characterized by IR spectroscopy and elemental analysis. Large single crystals suitable for X-ray single-crystal diffraction were obtained from the melt. The melting point was determined to be 38(±1) °C.

The preparation and properties of IL hydrogen sulfates have been previously described;[15] a different preparative protocol was employed in the present work. BDMIM[HSO_4] was prepared by reacting an equimolar mixture of sulfuric acid and silver sulfate in aqueous solution with a stoichiometric amount of BDMIMCl. After 12 h of stirring at ambient temperature, silver chloride was filtered from the solution and water was removed under reduced pressure at 110 °C. The remaining extremely viscous oil was recrystallized from MeCN/Et_2O (5:1) to yield colorless, slightly hygroscopic crystals suitable for X-ray single-crystal diffraction. The compound was characterized by NMR and IR spectroscopy and elemental analysis. The melting point was determined to be 78(±1) °C.

2.2. Elemental Analysis and Melting Points. The analysis of the metal contents was done by atomic absorption spectroscopy (AAS) using a Shimadzu 330 spectrometer. Carbon, hydrogen, and nitrogen contents were determined by standard elemental analysis using a CHNO-rapid analyzer (Heraeus). Chloride and bromide contents were determined by titration using the Volhard method. The melting points were measured using a Stuart Scientific SMP3 melting point apparatus.

2.3. Crystal Growth. Growing crystals of (BDMIM)$_4$[Fe^{II}-Cl_4][$Fe^{III}Cl_4$]$_2$ from the melt was performed in Schlenk tubes (∼10

(6) Wilkes, J. S.; Zaworotko, M. *J. Chem. Soc., Chem. Commun.* **1992**, 965.
(7) Tait, S.; Osteryoung, R. A. *Inorg. Chem.* **1984**, *23*, 4352.
(8) Abdul-Sada, A. K.; Al-Juaid, S.; Greenway, A. M.; Hitchcock, P. B.; Howells, M. J.; Seddon, K. R.; Welton, T. *Struct. Chem.* **1990**, *1*, 391.
(9) Hitchcock, P. B.; Seddon, K. R.; Welton, T. *J. Chem. Soc., Dalton Trans.* **1993**, 2639.
(10) Bonhôte, P.; Dias, A.-P.; Papageorgiou, N.; Kalyanasundaram, K.; Grätzel, M. *Inorg. Chem.* **1996**, *35*, 1168.
(11) Avent, A. G.; Chaloner, P. A.; Day, M. P.; Seddon, K. R.; Welton, T. *J. Chem. Soc., Dalton Trans.* **1994**, 3405.
(12) Suarez, S. E. P. A. Z.; Dullius, J. E. L.; de Souza, R. F.; Dupont, J. *J. Chim. Phys. Phys.-Chim. Biol.* **1998**, *95*, 1626.
(13) Huang, J.-F.; Chen, P.-Y.; Sun, I.-W.; Wang, S. P. *Inorg. Chim. Acta* **2001**, *320*, 7.
(14) Mele, A.; Tran, C. D.; De Paoli Lacerda, S. H. *Angew. Chem., Int. Ed.* **2003**, *36*, 4364.
(15) Wasserscheid, P.; Sesing, M.; Korth, W. *Green Chem.* **2002**, *4*, 134.
(16) Aggarwal, A.; Lancaster, N. L.; Sethi, A. R.; Welton, T. *Green Chem.* **2002**, *4* (5), 517.
(17) Ross, J.; Xiao, J. *Chem.—Eur. J.* **2003**, *9* (20), 4900.
(18) Dzyuba, S. V.; Bartsch, R. A. *J. Heterocycl. Chem.* **2001**, *38*, 265.

cm in length and ~1 cm in diameter) equipped with a septum through which a wire ending in a loop with seed crystals was immersed into the melt. The tubes were kept in a water bath maintained ~1 °C below the melting point. The crystals started growing at the loop, where they were separated from the melt typically after a couple of hours by slowly lifting the wire out of the liquid.

2.4. NMR and IR Spectroscopy. ^{1}H NMR and ^{13}C NMR spectra were recorded at ambient temperature using a Varian Mercury 200 spectrometer (200 MHz), with the ^{13}C spectra ^{1}H-decoupled. Chemical shifts where measured with respect to external standard tetramethylsilane (TMS).

IR spectra were recorded using a Nicolet FTIR spectrometer (model Avatar). The samples were diluted with thoroughly dried KBr and pressed into pellets or measured as liquids between KBr windows against a KBr background in the range from 600 to 4000 cm^{-1}.

2.4.1. 1-Butyl-2,3-dimethylimidazolium Chloride (BDMIMCl). ^{1}H NMR (200 MHz, CD_2Cl_2 solvent, ppm vs TMS): 1.0 t, C(11)-H_3; 1.4 t/t, C(10)H_2; 1.8 t/t, C(9)H_2; 2.8 s, C(8)H_3; 4.0 s, C(7)H_3; 4.2 t, C(6)H_2; 7.55 d, C(4)H; 7.9 d, C(5)H.

^{13}C NMR: 10.0, C(8); 14.0, C(11); 20.0, C(10); 33.0, C(9); 36.0, C(7); 49.0, C(6); 122.0, C(4); 124.0, C(5); 145.8, C(2).

IR (600−4000 cm^{-1}, KBr pellets): 3162, 3036, 3014 aromatic ν(C−H); 2964−2860 aliphatic ν_s(C−H); 1586 (s) ν_s(C═C/C═N) ring; 1420 (m) ν(C−H) Me; 1338 (w) δ_{as}(C−H) Me; 1244 (w) δ_{as}(C−H) ring; 1188 ν_s ring; 1115 (m), 1057 (w) δ(C−H) in-plane ring; 822 (m) δ(C−H) in-plane; 758 (m) δ_{as} out-of-plane ring; 669 δ_{as} ring.

Elemental analysis. C: calcd, 57.3%; found, 57.3%. H: calcd, 9.0%; found, 9.2%. N: calcd, 14.8%; found, 14.1%.

2.4.2. 1-Allyl-2,3-dimethylimidazolium Bromide (ADMIMBr). ^{1}H NMR (500 MHz, CD_2Cl_2 solvent, ppm vs TMS): 2.58 s, C(8)-H_3; 3.79 s, C(7)H_3; 4.95 d/t, C(6)H_2; 5.28 d/m, C(10)H−E; 5.38 d/m, C(10)H−Z; 5.98 m, C(9)H; 7.61 d, C(4)H; 7.73 d, C(5)H.

^{13}C NMR: 11.08, C(8); 27.69, C(6); 36.30, C(7); 120.65, C(9); 121.77, C(4); 123.22, C(5); 130.4, C(10); 144.66, C(2).

IR (600−4000 cm^{-1}, KBr pellets): 3169 (w), 3106 (m), 3056 (3014) (s), ν(C−H) aromatic/allyl; 2929−2860 ν_s(C−H) aliphatic; 1587 (s) ν_s(C═C/C═N) ring/allyl; 1411 ν(C−H) Me; 1344 (w) δ_{as}(C−H) Me; 1253 (s) δ_{as}(C−H) ring; 1170 ν_s ring; 1102 (m) δ(C−H) in-plane ring; 809 (s) δ(C−H) in-plane; 762 (m) δ_{as} out-of-plane ring; 675 δ_{as} ring.

Elemental analysis. C: calcd, 43.5%; found, 43.2%. H: calcd, 5.9%; found, 6.2%. N: calcd, 12.7%; found, 12.2%.

2.4.3. 1-Butyl-2,3-dimethylimidazolium Hydrogen Sulfate (BDMIM [HSO_4]). ^{1}H NMR (200 MHz, CD_2Cl_2 solvent, ppm vs TMS): 1.0 t, C(11)H_3; 1.4 t/t, C(10)H_2; 1.8 t/t, C(9)H_2; 2.6 s, C(8)-H_3; 3.9 s, C(7)H_3; 4.1 t, C(6)H_2; 7.3 d, C(4)H; 7.5 d, C(5)H; 10.1 s, HSO_4^-.

^{13}C NMR: 10.0, C(8); 14.0, C(11); 20.0, C(10); 32.0, C(9); 36.0, C(7); 49.0, C(6); 122.0, C(4); 124.0, C(5); 144.0, C(2).

IR (600−4000 cm^{-1}, KBr pellets): 3135 (s), 3107 (s), 3061 (s), 3040 (s) ν(C−H) aromatic; 2966−2870 ν_s(C−H) aliphatic; ≈2550 (broad) ν([HSO_4^-]$_2$); 1589 (s) ν_s(C═C/C═N) ring; 1421 (m) ν(C−H) Me; 1236 (w) δ_{as}(C−H) ring; 1167 (s) ν_s ring; 1115 (m), 1062 (w) δ(C−H) in-plane ring; 849 (s) δ(C−H) in-plane; 775 (m) δ_{as} out-of-plane ring; 671 δ_{as} ring; 583 $\nu_3(SO_4^{2-})$.

Elemental analysis. C: calcd, 43.4%; found 42.9%. H: calcd, 6.8%; found, 7.0%. N: calcd, 11.2%; found, 11.0%.

2.4.4. 1-Butyl-2,3-dimethylimidazolium Chloroferrate(II,III) ($(BDMIM)_4[Fe^{II}Cl_4][Fe^{III}Cl_4]_2$). IR (600−4000 cm^{-1}, KBr pellets): 3169 (w), 3129/3109 (s), 3078 (w) ν(C−H) aromatic; 2960−2848 ν_s(C−H) aliphatic; 1586 (m) ν_s(C═C/C═N) ring; 1422 (m) ν(C−H) Me; 1239 (m) δ_{as}(C−H) ring; 1139 (m), 1105 (w) δ(C−H) in-plane ring; 757 (s) δ_{as} out-of-plane ring; 670 δ_{as} ring.

Elemental analysis. C: calcd, 35.8%; found, 35.5%. H: calcd, 5.6%; found, 6.8%. N: calcd, 9.3%; found, 8.8%.

2.5. X-ray Structure Determinations. Single-crystal diffraction was performed on a Bruker diffractometer equipped with a graphite monochromator, a Smart-Apex CCD detector (Siemens), and Mo Kα radiation. A complete hemisphere was generally recorded in 600, 435, and 230 frames at ϕ angles of 0, 90, and 180°, respectively. Indexing was done using the program SMART, and frame integration and data reduction were done using the SAINT-PLUS suite. Absorption correction was performed using the program SADABS (all Bruker AXS). Sample crystals were filled into glass capillaries and sealed under argon atmosphere. Recording temperatures and crystallographic parameters for compounds **I**−**IV** are summarized in Table 1. Details of the structure determinations may be obtained from the Cambridge Crystallographic Database by quoting the depository numbers 221 798 (BDMIM[HSO_4]), 221 756 (BDMIMCl), 221 755 (ADMIMBr), and 221 757 ($(BDMIM_4)[Fe(II)Cl_4][Fe(III)Cl_4]_2$).

Table 1. Crystallographic Parameters for Compounds **I**−**IV**

	I	**II**	**III**	**IV**
space group	*Pbca*	$P2_1/n$	$P2_1/n$	$C2/c$
a (pm)	1360.2(3)	838.0(2)	783.4(2)	4060.0(8)
b (pm)	1052.5(2)	1171.0(2)	1113.7(2)	788.0(2)
c (pm)	1733.6(3)	1076.0(2)	1789.3(2)	1849.0(4)
β (deg)		90.74(3)	90.71(3)	102.69(3)
V (Å^3)	2481.8(1)	1055.8(2)	1037.5(3)	5771.0(5)
Z	8	4	4	4
fw (g/mol)	249.31	188.69	217.99	1716.12
D_c (g/cm^3)	1.334	1.187	1.390	1.975
T_{rec} (K)	213(1)	213(1)	295(3)	213(1)
R_1 ($F > 4\sigma(F)$)	0.054	0.064	0.045	0.054
wR_2 (all data)	0.145	0.176	0.125	0.181
GOF (F^2)	1.056	0.964	0.943	1.022

3. Results and Discussion

Compound **I** (BDMIM[HSO_4]) crystallizes in the orthorhombic space group *Pbca* with eight formula units per unit cell. The structure is built from double slices extending in the (100) plane, with orientations of the imidazolium cations alternating along the *a* axis such that it results in an antiparallel arrangement of butyl chains (Figure 1). The shortest contacts between the butyl chains are 390 pm (C(11)−C(6)) and 417 pm (C(9)−C(10)).

Two [HSO_4^-] ions, related by an inversion center, are connected by two short hydrogen bonds (261 pm) to form dimers with a cyclic [H−O−S−O···H−O−S−O···] charge-assisted hydrogen-bond arrangement. These dimers are also found along with hydrogen-bonded chains $(HSO_4^-)_\infty$ in the structure of $KHSO_4$ (d_{O-O} = 262 pm).[19,20] In addition, hydrogen bonding is also found between the HSO_4^- dimer and the two aromatic hydrogen atoms of the imidazolium ring (Figure 2). The donor−acceptor distances are 336 pm (C(5)−O(5)) and 323 pm (C(4)−O(3)), which results in H···O distances of 241 pm (H(3)···O(3)) and 245 pm (H(5)···O(5)) for the idealized hydrogen positions. Both

(19) Cotton, F. H.; Frenz, B. A.; Hunter, D. L. *Acta Crystallogr.* **1975**, *B31*, 302.
(20) Payan, F.; Haser, R. *Acta Crystallogr.* **1976**, *B32*, 1875.

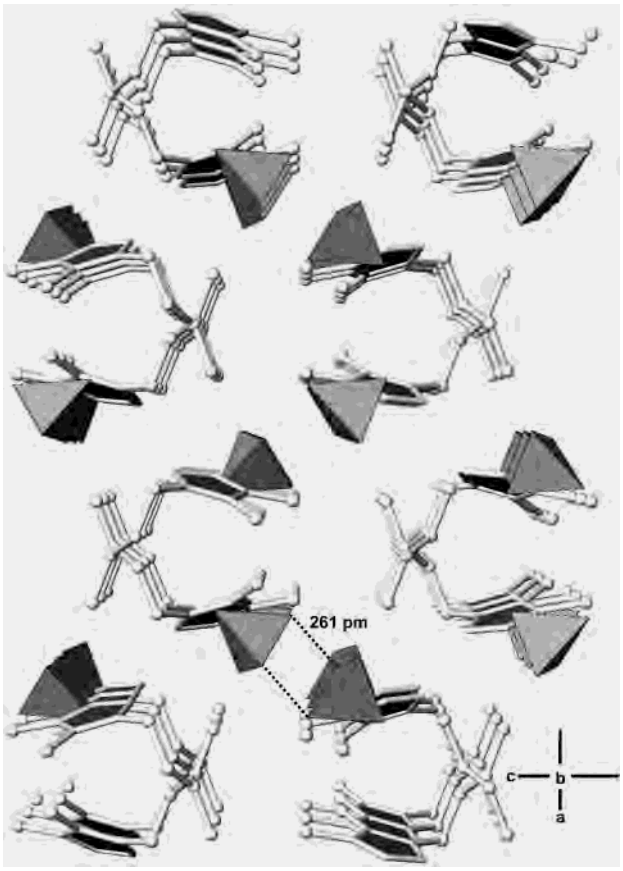

Figure 1. View into the crystal structure of BDMIM[HSO_4] along the *b* axis. [HSO_4^-] ions are shown as tetrahedra; the mode of dimer interconnection is indicated with dotted lines. All hydrogen atoms have been omitted for clarity.

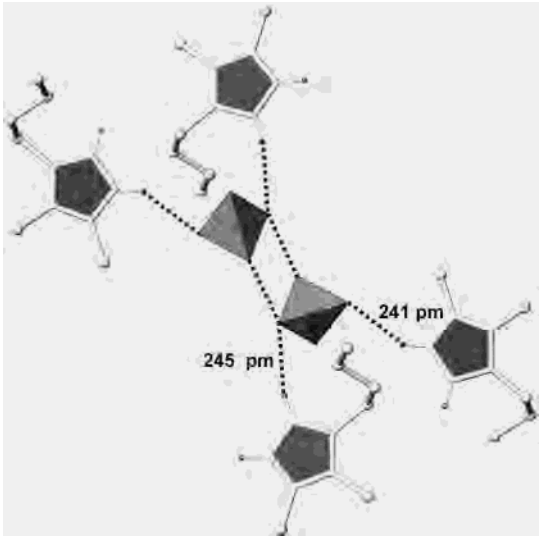

Figure 2. Surroundings of the [HSO_4^-]$_2$ dimer in the structure of BDMIM[HSO_4] with hydrogen bonds to the cations marked as dotted lines. All hydrogen atoms not involved in hydrogen bonding have been omitted for clarity.

contacts are well within the sum of the van der Waals radii ($r_H + r_O = 270$ pm); also, the C−H−O angles of 147° (C(4)−H(4)−O(3)) and 166° (C(5)−H(5)−O(5)) are indicative of strongly directional rather than purely electrostatic interaction.

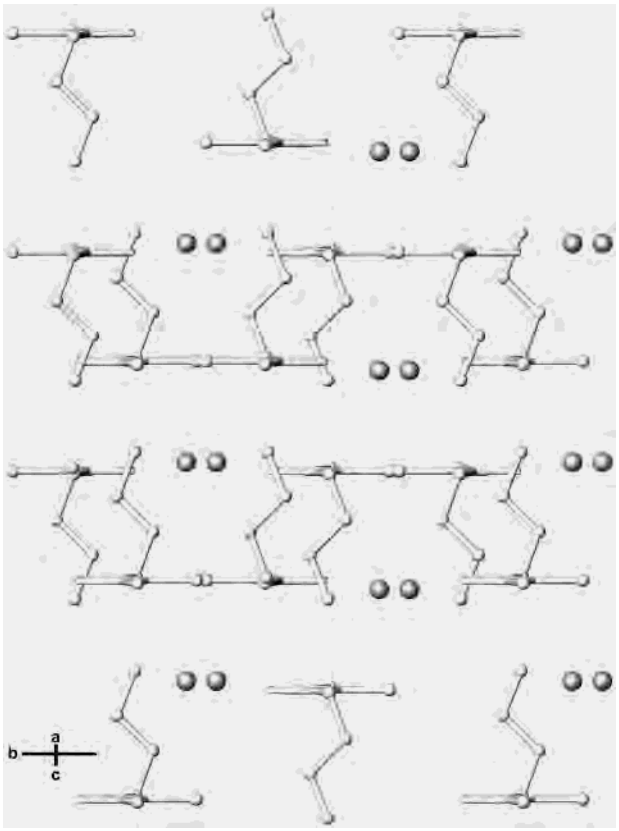

Figure 3. View into the crystal structure of BDMIMCl along the (101) direction. Chains of cations connected by chloride ions through hydrogen bonds run along the view direction. All hydrogen atoms have been omitted for clarity.

The IR spectrum of **I** also corroborates the presence of strong hydrogen bonds. Apart from a broad absorption with a maximum at ∼2550 cm^{-1}, originating from the [HSO_4^-] dimer, the two principal bands due to H(4) and H(5) are split into double bands with maxima at 3135/3107 cm^{-1} and 3061/3040 cm^{-1}, respectively. These bands are shifted to lower wavenumbers by ∼100 cm^{-1} with respect to the compound BDMIM[BF_4].

The single-crystal diffraction data of **II** (BDMIMCl) was sucessfully solved and refined with a monoclinic cell containing four formula units and space group $P2_1/n$. The structure is most conveniently described as being of the double-layer type with ring planes of the cations extending parallel to the $(10\bar{1})$ plane and the butyl chains stacked in an antiparallel arrangement perpendicular to this plane (Figure 3). The chloride ions are arranged in rows along the (101) direction, connecting the cations to form infinite hydrogen-bonded double chains. Each chloride is bound to two hydrogen atoms with (idealized) H···Cl···H angles of 157 and 168°, respectively, as shown in Figure 4a. Polarization by the chloride may cause deviations in the actual positions of the protons which cannot be accurately determined from the corresponding difference electron density maps.

A striking feature of the structure is shown in both Figures 3 and 4b. The ring planes are stacked pairwise along the *b* axis, with an interplanar distance of only 335 pm even though chlorides are *not* interconnecting cations of adjacent layers.

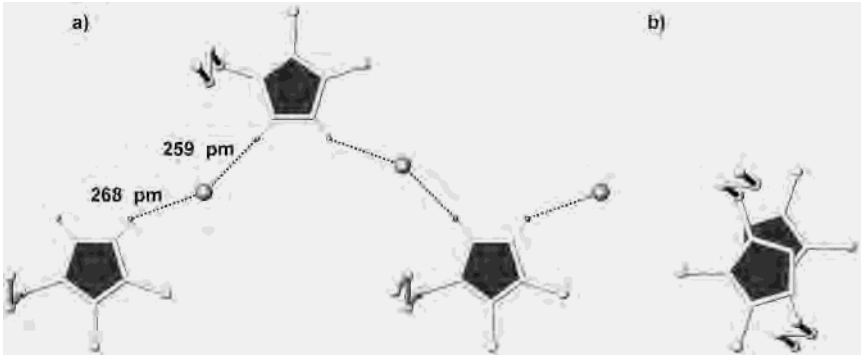

Figure 4. (a) Hydrogen-bonded double chain in the structure of BDMIMCl. Chloride ions are shown as gray spheres. All hydrogen atoms not participating in hydrogen bonding are omitted for clarity. (b) Stacking of the aromatic rings with an interplanar distance of 335 pm.

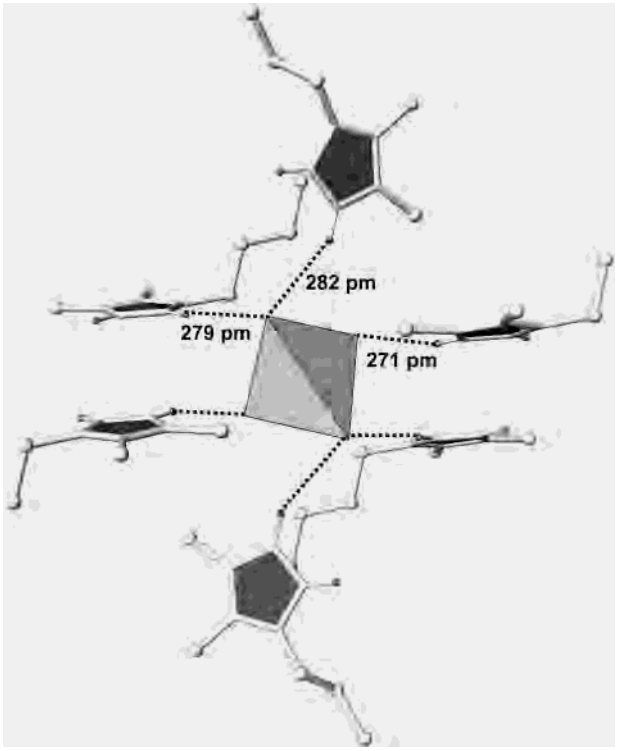

Figure 5. Surroundings of the $[FeCl_4^{2-}]$ ion in $(BDMIM)_4[Fe^{II}Cl_4][Fe^{III}Cl_4]_2$. All hydrogens not involved in hydrogen bonding are omitted for clarity.

The molecular dipoles in the direction of the ring plane are arranged in an antiparallel orientation. The structure could thus be regarded as being composed of ion-pair dimers of crystal chemical formula $[ImCl_{2/2}]_2$. Stacking of this type has apparently been observed before in the structure of EMIMCl·H_2O by Welton,[11] but the structural data was not published. The authors also found evidence for the existence of tightly hydrogen-bonded, quasi-molecular EMIMX species (X = halide) from NMR spectra and conductivity measurements of EMIM halide solutions in organic solvents. In these solutions, the cations show π-stacking interactions similar to those observed in the crystal structure in Figure 3. The strongly polarizing chloride ions obviously induce a shift of positive charge toward the aromatic hydrogens, thereby reducing the positive partial charges on the other atoms of the ring. The Coulombic repulsion between the cation is thus reduced, and the ring planes approach each other to a distance of twice the van der Waals radius of carbon. IR absorption bands of the aromatic hydrogens are found at 3036 and 3015 cm^{-1}; that is, the red shift by more than 150 wavenumbers with respect to that of the reference compound BDMIM-$[BF_4]$ is more pronounced than it is for **I**.

The same packing mode is observed in the structure of **III** (ADMIMBr), which possesses an allyl instead of a butyl chain at the imidazolium ring. The interplanar distance of the cation dimers is 345 pm, slightly larger than that in **II**.

Crystals of **IV** (BDMIM chloroferrate(II,III)) have been obtained from the melt using the experimental setup described above. Most of them are obtained as very brittle yellow rods and can be grown several centimeters in length under favorable conditions. Diffraction data were recorded at 213 K and at ambient temperature. The monoclinic cell found from indexing single crystals has a volume of 5771 $Å^3$, contains four formula units, and corresponds to space group *C*2/*c*. Most non-hydrogen atoms were located by difference Fourier synthesis. In two regions of the structure, however, the occurrence of disordered sites was evident. The first type of disorder is associated with the chloroferrate(III) ion and could be resolved at both 213 and 295 K.

The second type of disorder is associated with the butyl chain of one of the two crystallographically independent cations. This disorder has been resolved and corresponds to three different orientations of the chain at 213 K and also three orientations at 295 K, respectively. The region of butyl chain disorder can be located from Figure 6 in a layer of the structure where only one orientation of the chains with antiparallel stacking is shown. A section of this layer with a view perpendicular to the *b* axis, comprising three cations with different orientations of the butyl chain, is shown in Figure 7 for the low and ambient temperature structure.

The crystal structure can be rationalized from Figure 6 as being built from triple layers $(bab)_\infty$. The chloroferrate(II) ion is involved in hydrogen bonding to *all* cations with (idealized) H···Cl distances of 271, 279, and 282 pm, as depicted in Figure 5. The $[Fe^{II}Cl_4^{2-}]$ ions are at the center of hydrogen-bonded sheets extending in the (001) plane. One of the imidazolium ring planes, of which both hydrogen atoms are found to be involved in hydrogen bonding, is found with orientation parallel to this plane. Only one hydrogen

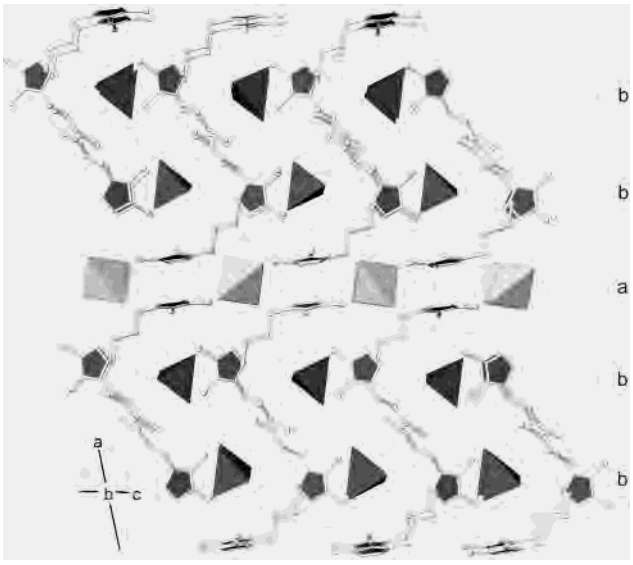

Figure 6. The structure of butyldimethylimidazolium chloroferrate(II,III) viewed along the *b* axis. Triple layers with the sequence BDMIM[$Fe^{III}Cl_4$]/$(BDMIM)_2[Fe^{II}Cl_4]$/BDMIM[$Fe^{III}Cl_4$] can be distinguished, with [$Fe^{II}Cl_4^{2-}$] shown as light gray tetrahedra and [$Fe^{III}Cl_4^{-}$] shown as dark gray tetrahedra. Only one of three orientations of the butyl chains is shown in the region between the triple layers.

bond is found with the second cation, namely, the one that has its ring plane oriented roughly perpendicular to the (001) direction.

The voids between the ring planes of the second cation are occupied by [$Fe^{III}Cl_4^{-}$] ions, whereas the disordered butyl chains extend to the margin of two adjacent triple layers. The pronounced anisotropy perpendicular to these triple layers, in terms of the molecular packing as well as the intermolecular forces, translates into the properties of the material. There is successively weaker intralayer bonding from the hydrogen-bonded region through the largely Coulombic [$Fe^{III}Cl_4^{-}$] region to the van der Waals layer of the butyl chains. The low melting point 311 K can be correlated with the regions of the low binding energy. Efficient packing of the butyl chains *between* the triple layers is obviously inhibited, as indicated by the pronounced disorder. The orientation of the outer cation is determined from its participation in strong hydrogen bonding to the [$Fe^{II}Cl_4^{2-}$] ion, which obviously precludes and energetically outweighs efficient packing of its butyl chains. The point is stressed with reference to a series of very low melting IL compounds with the BDMIM cation and fluoro anions, where disorder of the butyl chains has never been observed.[5] Consequently, van der Waals bonding in those compounds is comparatively strong, whereas it is rather weak as compared to the case of hydrogen bonds in the present case.

The crystals of **IV** are very brittle, in accord with a sheetlike structure. Moreover, rapid cooling of the melt results in a polycrystalline material, which shows texture reminiscent of liquid crystalline (LC) mesophases. The nature of this texture has not been investigated in detail, but LC behavior of long-chain imidazolium hexafluorophosphates at higher temperatures has been attributed to melting of the alkyl-chain sublattice. The present compound could indeed be supposed to exist in a semimolten state and somewhat schematically described as being composed of BDMIM[$Fe^{III}Cl_4$], which is liquid down to low temperatures, and $(BDMIM)_2[Fe^{II}Cl_4]$, which is a solid at ambient temperature (mp 334(1) K).

The IR spectrum of the compound is in accordance with those reported by Hitchcock et al., who distinguished three aromatic C−H vibrational bands in $EMIM_2[CoCl_4]$ and $EMIM_2[NiCl_4]$. Four aromatic C−H stretching vibrations of very different intensity are found at 3169 (w), 3129 (s), 3109 (s), and 3094 (w) cm^{-1} in the present compound. The red shift caused by hydrogen bonding, although much smaller than it is for the chloride compound, is evident as compared to the absorption bands observed in the vibrational spectrum of BDMIM[BF_4].[5] The spectrum is distinctly different from liquid BDMIM[$Fe^{III}Cl_4$] which shows one strong absorption at 3145 cm^{-1} and two weak absorptions at 3176 and 3085 cm^{-1} in the region of aromatic C−H stretching vibrations.

4. Conclusion

The three compounds discussed in this work elucidate the influence of C−H···X (X = O or Cl) hydrogen bonding in low temperature ionic liquid crystals. The topology of these bonds with respect to their contribution to lattice energies (reflected in the melting points) can be located in all structures and largely correlated with the acceptor strength of the anions. However, simple correlations between melting points, the charge density of the anions, and the number of C−H···X contacts cannot be devised. This is evident from the structures of EMIM[NO_3], including three short CH···O contacts per formula unit, mp 311 K, and BDMIM[HSO_4], with two short CH···O contacts per formula unit, mp 351 K. The formal charge density on the oxygen atoms is the same for both anions, and no significant hydrogen bonding with the cations is expected for either case, applying eq 1. The trend is similar for the respective chloride salts containing much stronger hydrogen bonds, with the difference in melting points, however, being only 16 K (EMIMCl melts at 357 K and BDMIMCl at 373 K). The higher melting points of the BDMIM salts in the previous two examples cannot be solely attributed to the cation, since the order is reversed in the respective hexafluorophosphate salts, with EMIM[PF_6] melting at 331 K and BDMIM[PF_6] at 313 K. Consequently, thermodynamic properties of ionic liquids are strongly dependent on the degree of *mutual fit* of the cation and the anion, in terms of size, geometry, and charge distribution. Strong hydrogen bonding in BDMIMCl to some extent compensates for the Coulombic repulsion between stacked, coplanar aromatic cations such that they approach each other to a distance of 335 pm. This is below the interplanar distance 340 pm observed in solid $C_6H_6 \cdot C_6F_6$, where the $\pi-\pi$ interaction is strongly attractive.[21] Ion pairing and formation of ion-pair dimers is usually observed in solutions of IL salts in solvents of medium polarity like dichloromethane. The packing scheme of the ions in **II** and **III** is reminiscent of such quasi-molecular building blocks.

(21) Overell, J. S.; Pawley, G. S. *Acta Crystallogr.* **1982**, *B38*, 1966.

Figure 7. Section of the structure of butyldimethylimidazolium chloroferrate(II,III) showing the disordered butyl chains at 213 K (left) and 298 K (right). Each of the three crystallographically equivalent cations is shown with a different conformation of the butyl chain. The site occupation factors for the three conformations have been refined.

The strong hydrogen bonds with chloride and bromide constitute a special case as compared to those of other hydrogen-bond-acceptor ions.

Experiments reported by Seddon et al. demonstrated a large increase in the viscosity of various ionic liquid melts containing the BMIM cation upon addition of small quantities of chloride.[22] Investigations of analogous compounds containing the even stronger hydrogen-bond acceptor, fluoride, should be a worthwhile issue in this respect. Although eq 1 clearly does not hold for oxo-anion acceptors ($[ClO_4^-]$ might be an exception), its validation for chlorometalates is strongly supported by the structure of BDMIM chloroferrate(II,III). The compound may be regarded as a true intermediate between liquid and solid IL salts, highlighting some of the features that superficially govern lattice energy. The effect of one hydrogen bond in the central part of the constituent triple layer energetically outperforms the disfavorable effect on alkyl packing at the periphery. The exceptional energetic contribution of hydrogen bonding as compared to Coulombic and dispersive forces is reflected in the sheet structure comprising alternating layers of strongly interconnected $BDMIM_2[Fe^{II}Cl_4]$ units and weakly bound $BDMIM[Fe^{III}Cl_4]$ units. If present, hydrogen bonding is by far the most important contribution to the lattice energy in IL compounds. Mixing of appropriate constituents in tailor-made ionic liquids could involve hydrogen-bonding species (if these are desirable for a certain application) and non-hydrogen-bonding species in order to lower the melting point of the mixture. Furthermore, the chloroferrate example might suggest a guideline for designing the properties of *anisotropic* materials by combining tight binding molecular components (hydrogen-bond-donor/acceptor pairs) with considerably weaker Coulombic and dispersive interactions. If the constituents of those materials are ions rather than molecules, largely employed in crystal engineering, properties such as ionic conductivity and possibly even intercalation of guest molecules could be selectively addressed.

Acknowledgment. The financial support provided by the Fonds der Chemischen Industrie is gratefully acknowledged.

Supporting Information Available: X-ray crystallographic data in CIF format for the structure determinations of $BDMIM[HSO_4]$, BDMIMCl, ADMIMBr, and $(BDMIM_4)[Fe^{II}Cl_4][Fe^{III}Cl_4]_2$. This material is available free of charge via the Internet at http://pubs.acs.org.

IC035237L

(22) Seddon, K. R.; Stark, A.; Torres, M.-J. *Pure Appl. Chem.* **2000**, *72*, 2275.